

Optical Properties and London Dispersion Forces of Amorphous Silica Determined by Vacuum Ultraviolet Spectroscopy and Spectroscopic Ellipsometry

Guo-Long Tan,^{*,†} Michael F. Lemon,[‡] and Roger H. French^{*,†,‡}

Department of Materials Science and Engineering, University of Pennsylvania, Philadelphia, Pennsylvania 19104

DuPont Central Research, E356-384 Experimental Station, Wilmington, Delaware 19880

Precise and accurate knowledge of the optical properties of amorphous silica is important because of the increasing application of SiO₂ in optical and electrooptical devices, including photolithography masks for semiconductor fabrication, recently as a potential 157 nm mask substrate. The optical properties in the vacuum ultraviolet (VUV) region have been investigated, because they convey detailed information on the electronic structure and interatomic bonding of the material. In this work, we have combined spectroscopic ellipsometry and VUV spectroscopy to directly determine the optical functions of SiO₂ in this range, thereby reducing the uncertainty in the low-energy extrapolation of the data, essential for Kramers–Kronig analysis of VUV reflectance. We report the complex optical properties of SiO₂, over the range of 1.5 to 42 eV, showing improved agreement with theory when contrasted with earlier results. In addition to the features previously reported at 10.4, 11.6, 14.03, and 17.10 eV, new interband transitions have been observed at 21.3 eV along with O 2s transitions at 32 eV. We found the bulk plasma peak to be 23.7 eV in the energy loss function spectrum. Based on the magnitude of these new results, the Hamaker constant for SiO₂|Vacuum|SiO₂ is 71.6 zJ, which is larger than the previously reported value of 66 zJ.

I. Introduction

SILICON DIOXIDE is a material of considerable technological importance, with broad application in devices containing optics, optical fibers, and microelectronics such as metal oxide semiconductor transistors, etc.¹ It also forms the basis for the glass matrix used to encapsulate radioactive waste material. It exists in many crystalline forms, the better known being quartz, cristobalite, tridymite, stishovite, and coesite, but its best-known form is amorphous silicon dioxide. This form can be fabricated in the purest state and is the most widely used technologically. With the exception of stishovite, which is a rare form of SiO₂, the basic structural unit in all these forms of SiO₂ is the same, a SiO₄ tetrahedron. Each silicon atom is tetrahedrally coordinated with four oxygen atoms and each oxygen atom serves as a bridge connecting two tetrahedra.² The various forms of SiO₂ are obtained by linking the tetrahedra together in different ways. The two forms that are the most common and the most studied are

crystalline α -quartz and amorphous SiO₂. These are also the forms that are structurally quite similar. In α -quartz the Si–O bond length is 1.61 Å and the Si–O–Si angle is 144°. In amorphous SiO₂ these two parameters have random distributions, but their mean values are about the same as in α -quartz. The tetrahedron, on the other hand, remains almost perfect with only very small deviation in the O–Si–O angle of 109.5° in α -quartz.⁴ It is known that Suprasil 1 OH-containing glass possesses a more ideal glass structure with a narrower distribution of Si–O bond lengths or Si–O–Si bond angles. Insight into how glass structure impacts the band gap energy of fused silica is provided by the work of Ching, who has calculated band structures for a family of crystalline SiO₂ compounds including the variation of the band gap energy with structural parameters such as the Si–O bond length and the Si–O–Si bond angle.⁵ In SiO₂, the Si–O–Si bond lengths vary from 1.55 to 1.65 Å while the bond angles vary from ~136° to 180° and these changes are found to correlate to changes in the band gap energy from 8.4 to 11 eV.⁶ The experimentally determined direct band gap energy of fused SiO₂ ranges from 7.52 eV ($\alpha = 14 \text{ cm}^{-1}$)⁷ to 9.6 eV ($\alpha = 4 \times 10^5 \text{ cm}^{-1}$),⁸ depending on measurement method, definition, analysis, OH contents, and defects inside the glass.

The continuous challenge for optical lithography in semiconductor device fabrication is to produce ever-smaller feature sizes. This requires the use of light sources with ever-shorter wavelengths for optical lithography. The research front has shifted from ArF excimer laser wavelength (193 nm or 6.425 eV) to F₂ laser wavelength (157 nm or 7.87 eV).^{9,10} Changing the exposure wavelength from 193 to 157 nm imposes severe requirements on the optical materials, including high transmittance and extremely good uniformity over a large volume at 157 nm. These requirements are not satisfied by the currently available materials. For instance, amorphous silica, which is widely used in KrF and ArF excimer laser lithography, requires modification to have sufficient transparency to be applicable to F₂ laser lithography. The band gap energy of amorphous SiO₂ remains somewhat controversial because of different definitions and fitting methods, but the fundamental absorption edge attributed to electronic transition of the Si–O–Si network has been reported to be at around 9 eV¹¹ by photoconductivity measurement, which is corresponding to the direct band gap of amorphous SiO₂ and is significantly higher than that of F₂ laser light at 7.9 eV, while the direct band gap of Suprasil 1 SiO₂ glass containing OH was reported to be 7.52 eV.⁷ The type of modification needed to improve the transparency of fused silica glass at 157 nm has been recently demonstrated by Hosono and co-workers,^{12,13} and Moore and Smith,^{14,15} who have shown that the doping of fluorine and the reduction of SiOH content in synthesized silica glass, which is called “modified fused silica,” results in a dramatic improvement in optical transmission at 157 nm and in durability to F₂ laser irradiation. The fluorine doping is thought to produce a “chemical annealing” by the reduction of strained Si–O–Si bonds. Since then, modified silica glass has been evaluated as one of the primary candidate materials for optical transmission components in F₂ lithography, especially

B. Dunn—contributing editor

Manuscript No. 186563. Received November 3, 2002; approved June 12, 2003. This work was partially funded by NSF Award DMR-0010062 in cooperation with EU Commission Contract No. G5RD-CT-2001-00586.

^{*}Member, American Ceramic Society.

[†]University of Pennsylvania.

[‡]DuPont Central Research.

for photomask substrates. Therefore, amorphous silica continues as the focus of much fundamental research to understand its electronic structure, bonding characterization, defects, and optical properties.

Optical properties of crystalline and noncrystalline SiO₂ in the spectral range 0–26 eV were investigated 20 years ago by Phillip.^{16–19} He observed identical optical properties for crystalline and fused quartz and found the spectral dependence of the real and imaginary parts of the dielectric function on composition value of x for SiO _{x} ($x = 0–2$). The spectral region of 5–40 eV has been studied by Sorokin.²⁰ Pantelides²¹ compared optical and theoretical absorption spectra of SiO₂ and then concluded that electron–hole interactions not only produce an exciton at 10.4 eV, but also substantially modify the interband continuum. He assigned the 10.4 eV peak to excitonic resonances rather than interband transitions. Also, Bosio *et al.* determined the same optical properties for *c*-SiO₂ and *a*-SiO₂.²² Meanwhile, Tarrío and Schnatterly reported similar optical properties for *cvd*-SiO₂ thin films derived from electron energy loss spectrum, evaporated SiO₂ films, and bulk silica.²³ This has been confirmed by many later studies,^{24,25} leading to the conviction that optical spectra in all SiO₂ phases with 4:2 coordination are quite similar.

Because high-purity synthetic SiO₂ glasses show promise as photograph mask substrates for 157 nm F₂ laser lithography, we have undertaken the measurement of the vacuum ultraviolet (VUV) optical spectra of amorphous SiO₂, from which we determine the optical functions n and k , ϵ_1 and ϵ_2 , as well as interband transition strength (J_{cv}). In previous work, our group used VUV spectroscopy²⁶ over the photon energy range of 2 to 40 eV to study the electronic structure of aluminum nitride. Here, we augment the VUV reflectance measurements with spectroscopic ellipsometry measurements over the range of 0.69 to 8.0 eV. A procedure for simultaneously performing Kramers–Kronig dispersion analysis on the data from these two sources was described previously.²⁷ Using the augmented data spanning a wider energy range leads to improved accuracy in amplitude, affording greater precision in determining the quantitative optical properties of SiO₂.

II. Experimental Methods

(1) Sample Preparation

The amorphous SiO₂ sample studied here is of Suprasil 1 glass.²⁸ Suprasil 1 is among the highest purity and most homogeneous of commercial SiO₂ glasses. The samples were synthesized from high-purity raw materials and contain less than a total of 1 ppmw metallic impurities. The type 1 grade of Suprasil is essentially isotropic for index variations. Suprasil 1 is made using a flame torch, which leads to an OH content in the final glass of 1200 ppmw. This glass is practically free from bubbles and inclusions, homogeneous, and free from striae in all directions and characterized by a very high optical transmission in the UV and visible spectral ranges. The sample was polished on both faces for spectroscopic ellipsometry and VUV optical measurement.

(2) Spectroscopic Ellipsometry

Spectroscopic ellipsometry was performed with the VUV-Vase instrument,²⁹ which has a range from 0.69 to 8.55 eV (1800 to 145 nm), and employs MgF₂ polarizers and analyzers rather than the more common calcite optics. The instrument has a MgF₂ autoretarder and is fully nitrogen purged. The spot diameter at the sample is 2 mm. The instrument measures the ellipsometric parameters Ψ and Δ , defined by Eq. (1),

$$\tan(\Psi)e^{i\Delta} = \frac{R_p}{R_s} \quad (1)$$

where R_p/R_s is the complex ratio of the p- and s-polarized components of the reflected amplitudes, with R_p and R_s representing the electric field components parallel (p) and perpendicular (s) to the plane of incidence, respectively. In these measurements, the

light was incident on the front surface of the sample at angles of 60°, 70°, and 80° relative to the surface normal. These parameters are analyzed using the Fresnel equations³⁰ in a computer-based modeling technique to directly determine a material's optical functions.

(3) VUV Spectroscopy

VUV spectroscopy is an established technique for electronic structure studies of materials. It has the advantage of covering the complete energy range of the valence interband transitions³¹ and is unaffected by the sample charging that attends photoelectron spectroscopy on insulators. The VUV spectrophotometer employs a laser plasma light source, monochromator, and filters.³² The details of the instrument have been discussed previously.^{32,33} The energy range of the instrument is from 1.7 to 44 eV, or from 700 to 28 nm, and extends well beyond the air-cutoff of 6 eV and the window-cutoff of 10 eV. The resolution of the instrument ranges from 0.2 to 0.6 nm, which corresponds to 16 meV resolution at 10 eV or 200 meV resolution at 35 eV.

(4) Hamaker Constant Calculations

Once the optical properties and electronic structure of bulk amorphous SiO₂ have been determined, then the full spectral Hamaker constant³⁴ can be determined using the Lifshitz method, as has been described elsewhere.³⁵ For the case of two grains of material 1 which are separated from each other by an intervening intergranular material (material 2), then the Hamaker constant, A_{121}^{NR} , determines the magnitude of the van der Waals force between the two grains. The intergranular material serves to shield the attraction of the two materials. The Hamaker constant is large for a vacuum interlayer, and is zero if the interlayer material 2 is identical to the layer's material 1. The relationship between Hamaker constant and van der Waals force is expressed as follows:

$$A_{121}^{NR} = -6\pi L^3 F_{vdW} \quad (2)$$

To calculate the London dispersion force, the major component of the van der Waals forces, we use another Kramers–Kronig dispersion relation to produce the London dispersion spectrum, $\epsilon_2(\xi)$, which is an integral transform of the imaginary part of the dielectric function from one of real frequency ω to one of imaginary frequency ξ . The London dispersion spectrum is a material property and represents the retardation of the oscillators.

$$\epsilon_2(\xi) = 1 + \frac{2}{\pi} \int_0^\infty \frac{\omega \epsilon_2(\omega)}{\omega^2 + \xi^2} d\omega \quad (3)$$

Once the London dispersion spectra of the two materials are determined, the Hamaker constant is calculated using integrals of spectral differences.³⁵

III. Results

(1) Analysis of Ellipsometry Data

The ellipsometric results for Suprasil 1 amorphous SiO₂ are shown in Fig. 1. The transmission of the Suprasil 1 amorphous SiO₂ within the deep ultraviolet (DUV) range measured on an ellipsometer is shown in Fig. 2. To determine the optical functions of the bulk amorphous SiO₂ samples, we use both ellipsometric and UV/vis transmission data taken on the same sample to find a solution of the model describing the optical behavior of the bulk amorphous silica.³⁰ Using transmission data simultaneously with ellipsometric data in the ellipsometric modeling reduces the effective surface sensitivity of ellipsometry, while increasing the accuracy of the bulk properties such as the extinction coefficient. Our complex index of refraction within the energy range of 0.7 to 8 eV for this solution is shown as continuous lines in Fig. 3, which fits very well with Philipp's results,³⁶ shown as circle and triangle symbols within the energy range of 0.75–6 eV.

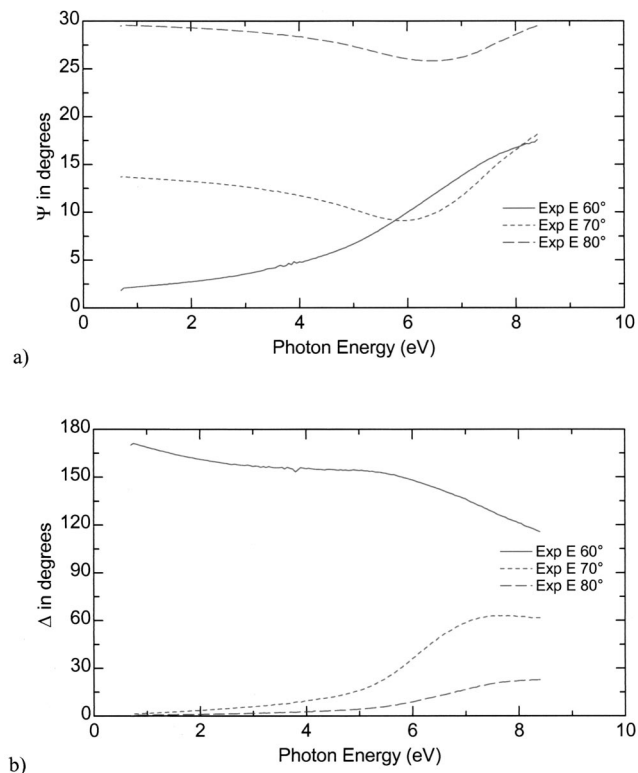


Fig. 1. Ellipsometric data (a) Ψ and (b) Δ for Suprasil 1 amorphous SiO₂. "Exp E" refers to the angle of incidence of the experimental data.

(2) Kramers–Kronig Analysis of VUV Reflectance

The VUV reflectance data used in this work is reported in Fig. 4. By augmenting the raw VUV reflectance data with ellipsometric results, we obtain more accurate results for the quantitative optical properties as exhibited in Fig. 4. The reflectance as a function of energy ($R(E)$) is appropriately scaled and augmented by extending the reflectance data outside the VUV experimental range, appropriately fitting low and high energy wings. Kramers–Kronig analysis is then used to recover the reflected phase. In the case of

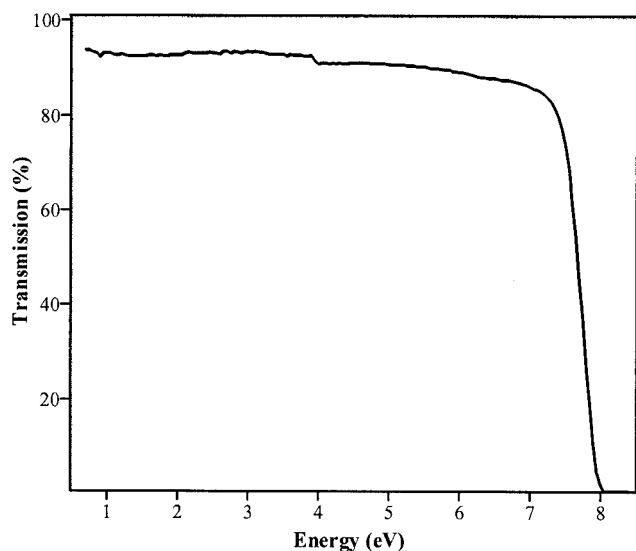


Fig. 2. Transmission of Suprasil 1 amorphous SiO₂.

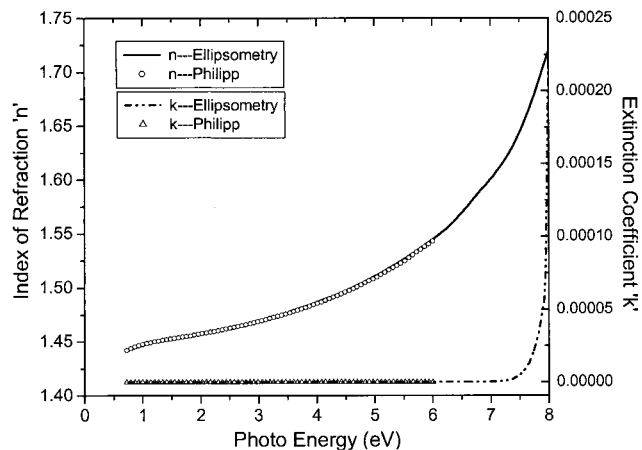


Fig. 3. Complex index of refraction, $\hat{n} = n + ik$, determined for Suprasil 1 amorphous SiO₂; the index of refraction, n , is shown as a solid line, while the extinction coefficient, k , is shown as a dashed line.

normal incidence, the complex reflection coefficient is written in terms of the amplitude $|\tilde{R}|$ and a phase shift on reflection θ , as described by

$$\tilde{R} = |\tilde{R}|e^{-i\theta} = \frac{n - 1 - ik}{n + 1 - ik} \quad (4)$$

The absorption coefficient, α , in units of cm^{-1} for Suprasil 1 amorphous SiO₂ is shown in Fig. 5. In the region of the fundamental absorption edge, the dashed line was calculated from the VUV spectrum and the square-symbol line was calculated from ellipsometric spectroscopy data within the low energy range. The complex index of refraction ($\hat{n} = n + ik$) for Suprasil 1 amorphous SiO₂ is then calculated algebraically from Eq. (4) and the results are shown in Fig. 6, while the dielectric function is obtained from the relation $\epsilon_1 + i\epsilon_2 = (n + ik)^2$ and is shown in Fig. 7. Obviously it can be seen from Fig. 6 that the index of refraction and extinction coefficient values measured from spectroscopic ellipsometry (short course curves) agree with those calculated from VUV data through Kramers–Kronig analysis within the 0.7–8 eV energy

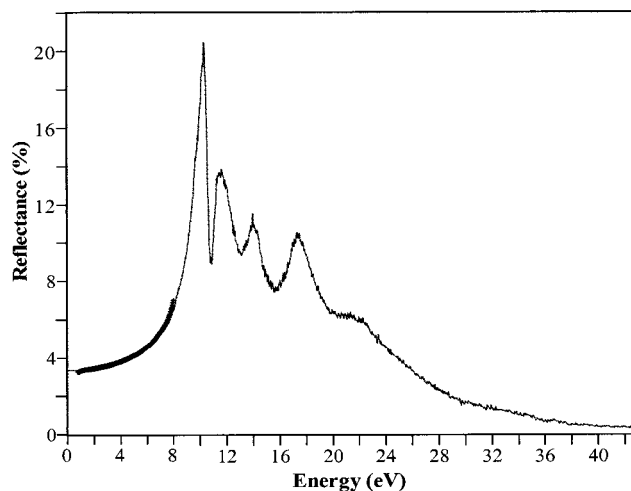


Fig. 4. Reflectance of Suprasil 1 amorphous SiO₂; the dashed line is measured from VUV spectrum and the short solid line from spectroscopy ellipsometric data.

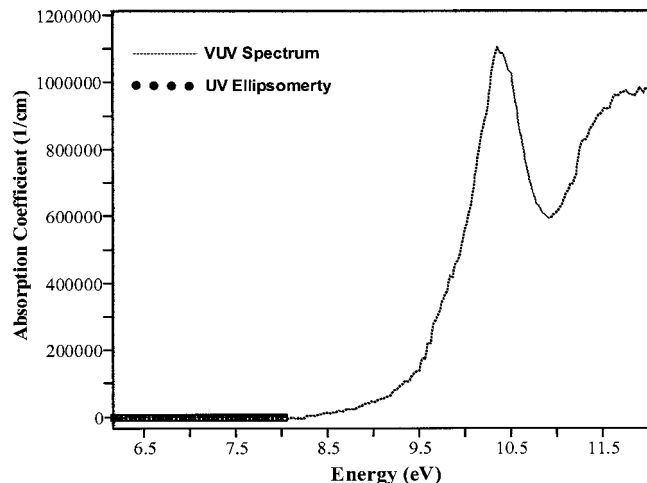


Fig. 5. Fundamental absorption edge of Suprasil 1 amorphous silica. The absorption coefficient (α), in units of cm^{-1} , is plotted versus energy. The dashed line represents absorption coefficient derived from VUV spectrum; the short course line from ellipsometry spectroscopy.

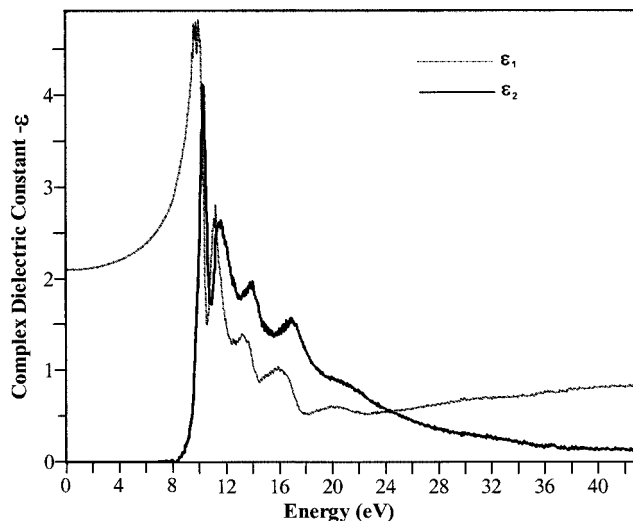


Fig. 7. Complex dielectric constant of Suprasil 1 amorphous SiO_2 , where the real part, ϵ_1 , is shown by the dashed line and the imaginary part, ϵ_2 , by the solid line.

range, indicating that the index of refraction from VUV data could also agree with Philipp's result³⁶ for $a\text{-SiO}_2$ very well, as shown in Fig. 3. Here we render the optical response in terms of the interband transition strength, $J_{cv}(E)$, related to $\epsilon(\omega)$ by

$$J_{cv}(E) = \left(\frac{m_0^2}{e^2 \hbar^2}\right) \left(\frac{E^2}{8\pi^2}\right) [\epsilon_2(E) + i\epsilon_1(E)] \quad (5)$$

where $J_{cv}(E)$ is proportional to the transition probability and has units of $\text{g}\cdot\text{cm}^{-3}$. For computational convenience we take the prefactor $m_0^2 e^{-2} \hbar^{-2}$ in Eq. (2), whose value in cgs units is $8.289 \times 10^{-6} \text{g}\cdot\text{cm}^{-3}\cdot\text{eV}^{-2}$, as unity. Therefore, the $J_{cv}(E)$ spectra calculated from Eq. (5) shown in Fig. 8 are in units of eV^2 .

Applying the oscillator strength sum rule³⁷ for the interband transition strength, $n_{\text{eff}}(E)$, the number of electrons contributing to a transition up to an energy E , is

$$n_{\text{eff}}(E) = \frac{4v_f}{m_0} \int_0^E \frac{J_{cv}(E')}{E'} dE' \quad (6)$$

where v_f is the volume of the SiO_2 formula unit, 45.3 \AA^3 . The effective number of electrons participating in interband transitions at energies less than or equal to the photon energy, E , based on the oscillator strength sum rule, is displayed for Suprasil 1 amorphous SiO_2 in Fig. 9.

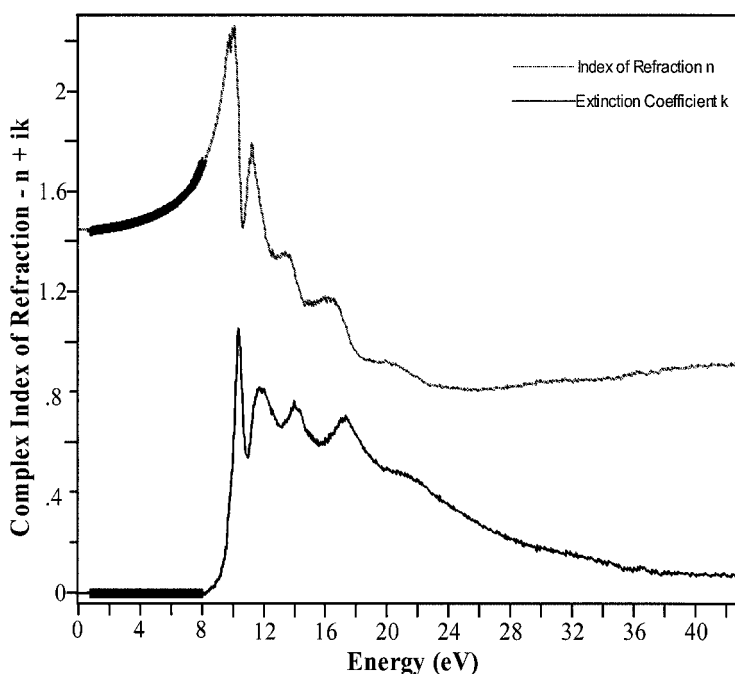


Fig. 6. Complex index of refraction of Suprasil 1 fused SiO_2 , where the index of refraction, n , is shown by the dashed line and the extinction coefficient, k , by the solid line.

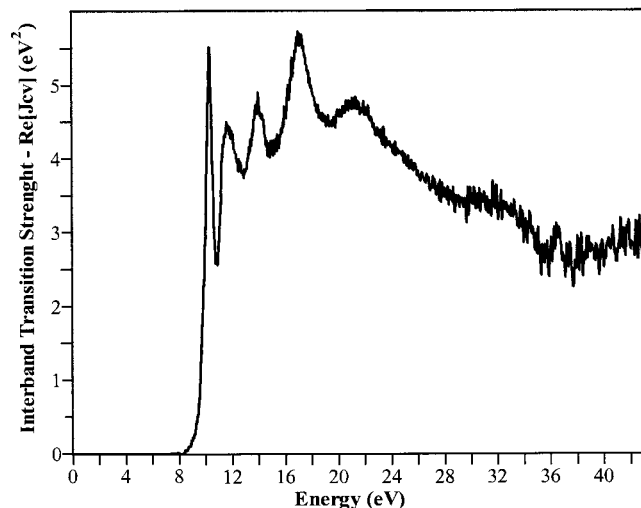


Fig. 8. Real part of the interband transition strength ($\text{Re}[J_{cv}]$) of Suprasil 1 amorphous SiO_2 determined from Kramers–Kronig analysis of VUV reflectance data.

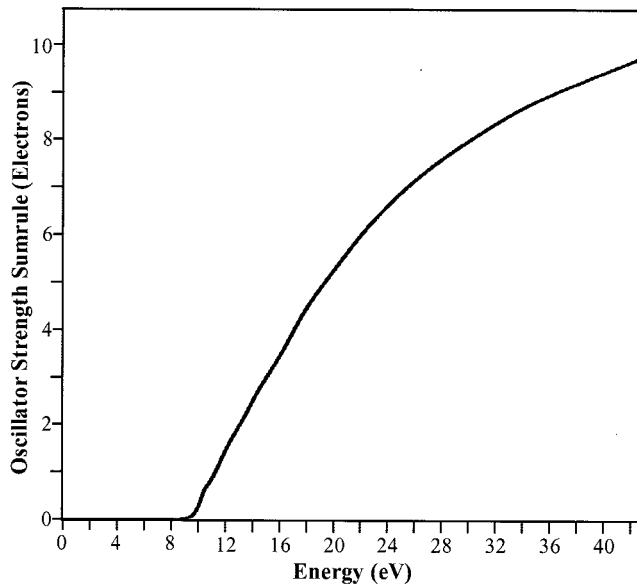


Fig. 9. Oscillator strength sum rule of Suprasil 1 amorphous SiO_2 .

IV. Discussion

(I) Optical Properties of Suprasil 1 SiO_2

(A) *Band Gap*: Reflectance values for Suprasil 1 amorphous SiO_2 are shown in Fig. 4, which agree qualitatively with the reported optical transitions in other crystalline and amorphous silica.^{16,17,20,21} It can be seen from Fig. 4 that the reflectivity peaks are located at 10.4, 11.6, 14.03, and 17.10 eV, respectively, as reported previously. The experimentally determined absorption coefficient, α (cm^{-1}), calculated from its reflectance spectrum for Suprasil 1 SiO_2 fused glass, is shown in Fig. 5 in the energy region of the absorption edge. The absorption is dramatically decreased below 9.2 eV for Suprasil 1 fused silica. In Table I the results of direct and indirect band gap fittings are summarized for three different ranges of the absorption coefficients. A band gap energy is determined using a direct gap model using a linear fit in the region of interest to a plot of $\alpha^2 E^2$, where α is the absorption coefficient in cm^{-1} and E is energy in eV. A band gap energy for an indirect band gap model is determined by linear fitting to $\alpha^{1/2}$. Formally direct and indirect band gap models do not apply to amorphous materials such as glass, due to the loss of long-range periodicity in the amorphous material, and the consequent destruction of the Brillouin zone construct used for band structure analysis. Here we are using the direct and indirect models only as a tool to characterize the complex absorption edge behavior of the sample, and draw on the crystalline band gap models because the shapes of the absorption edges measured are reminiscent of those found in crystalline materials.³⁸ The direct and indirect gap fitting has been used previously for characterizing the changes in the absorption edge in amorphous materials such as silicon³⁹ and other amorphous semiconductors⁴⁰ and has been found useful to characterize the observed changes in the electronic structure. The evaluated direct gap for Suprasil 1 amorphous SiO_2 in the upper limit is about 9.9 eV corresponding to $\alpha = 5.6 \times 10^5 \text{ cm}^{-1}$, which is similar to Ravindra's result,⁸ while the indirect gap in this region is evaluated to be 8.9 eV. Within the absorption region of

2.5×10^5 to $5.6 \times 10^5 \text{ cm}^{-1}$, the direct band gap was fitted to be 9.55 eV from the absorption edge. Also the band gaps of Suprasil 1 fused SiO_2 in the region of low absorption coefficient (31–1436 cm^{-1}) have been calculated from both VUV and ellipsometric spectra to be 7.92 eV for direct transition and 7.72 eV for indirect transition, respectively, which are close to French's evaluation results.⁷ This direct gap evaluated in the low absorption region is comparable to the transparent cutoff value at 7.87 eV as shown in Fig. 2. Weinberg *et al.*⁴¹ as well as DiStefano and Eastman⁴² have reviewed other experimental determinations of the direct band gap of SiO_2 and reported values of 9.3 and 9.0 eV, respectively, for the band gap of SiO_2 from photoconductivity measurements. These values are 1.08–1.38 eV higher than the band gap of Suprasil 1 amorphous SiO_2 determined in the region of low absorption coefficients here. The reason for the difference is that Suprasil 1 fused silica has very high OH content (up to 1200 ppmw level), which produces a substantial quantity of $2\equiv\text{Si}-\text{OH}$ as discussed by Griscom.⁴³ This Si–OH group may play an important role in altering the direct band gap energy for OH-containing fused glass. With the presence of the Si–OH group, the band gap of fused SiO_2 decreases with increased OH content.⁷ Meanwhile, absorption of the bulk specimen at around 7.9 eV has several origins including extrinsic impurities, intrinsic defects including oxygen-deficient centers (ODCs), and strained Si–O–Si bonds in three- or four-member rings.⁴⁴

(B) *Interband Transitions*: In addition, we observed two new interband transition peaks in the interband transition strength ($\text{Re}[J_{cv}]$) of Suprasil 1 amorphous SiO_2 (as shown in Fig. 8) at 21.3 and 32 eV. The optical properties of SiO_2 below 11 eV have been the subject of considerable interest and controversy.⁴⁵ Laughlin⁴⁶ conducted a detail study of the optical-absorption spectrum of SiO_2 . According to his calculations, the peak at about 10.4 eV in Fig. 8 could be assigned to excitonic resonance. Actually the sharp peak at 10.4 eV was also identified to be excitonic by many other

Table I. Results of Band Gap Fitting from VUV Absorption Edge for Suprasil 1 Fused Silica

Sample	Direct gap (eV)	Abs. fitting range (cm^{-1})	Indirect gap (eV)	Abs. fitting range (cm^{-1})
Suprasil 1	7.92 [†]	31–1436	7.72 [†]	13–1293
Amorphous SiO_2	9.55	2.5×10^5 – 5.6×10^5	8.30	2.4×10^4 – 1.7×10^5
	9.90	5.6×10^5 – 1.1×10^6	8.90	1.3×10^5 – 1.1×10^6

[†]Calculated from ellipsometric spectroscopy.

authors.^{17,20,21,23,24,47} Obviously, as reported in many early papers, the other three features of the spectrum at 11.6, 14.03, and 17.10 eV are due to interband transitions, which agree in energy with the measurements of other authors.^{16,18,23} By following Ibach's conclusion,⁴⁸ the 11.6 eV transition corresponded to an excitation from the valence band maximum at -12.9 eV to the conduction band edge. The remaining 14.03, 17.3, 21.3, and 32 eV features may be assumed to originate from the three principal maxima in the valence band density of states and the O 2s core state, respectively, terminating on an exciton lying ~ 1.3 eV below the conduction band edge.⁴⁵ Specifically, these different interband transitions could be assigned from the band structure⁴⁵ of SiO₂ as follows: the feature at -14.03 eV is for the transition from the energy level at 14.3 eV in valence band (VB) to the energy level at -0.27 eV in conduction band (CB); the feature peak at 17.4 eV is for the transition from -16.9 eV to CB 0.5 eV; the feature peak at 21.3 eV is for the transition from VB -20.1 eV to CB 1.2 eV; and the 32 eV feature peak is for the transition from O 2s core level at -30.6 eV to a low-lying vacant state near the CB edge.

Ibach and Rowe⁴⁸ studied the electronic structure of oxygen adsorbed on silicon (111) surfaces and oxidized silicon by electron energy loss spectroscopy; they observed bulk plasma loss peak at 21.3 eV and two additional interband transition features peaks at 23 and 32 eV. Similar feature peaks at 21.3 and 32 eV have also been observed in our measurement as shown in Figs. 4 and 8, and have never been reported in optical spectra before. The broad feature peak at 21.3 eV could be assigned as either due to interband transitions or the bulk plasma resonance. In the former case, it would correspond to electronic transitions from the oxygen valence band at -20.1 eV to the conduction band state at 1.3 eV, which is supported by Xu and Ching's *ab initio* calculation of optical properties of SiO₂.⁴⁸ In the latter case, it is tempting to assign this feature to the same plasmon resonance, as discussed in the valence electron energy loss spectrum (EELS).⁵⁰ To confirm that the feature peak at 21.3 eV arises from the plasmon resonance of SiO₂, we have calculated the energy loss function (ELF = $-\text{Im}[1/\epsilon(\omega)]$) (shown in Fig. 10) using the complex dielectric function (shown in Fig. 7), which has been extracted from Kramers-Kronig analysis of our measurements. Our energy loss function, shown in Fig. 10, is limited to 45 eV while the valence EELS extends to 100 eV. The bulk plasmon peak in the ELF spectrum is observed at 23.7 eV. Similar ELF data have been obtained by Maixner *et al.*,⁵¹ whose results for amorphous SiO₂ in small wave vector ($q = 0.2$) are in good agreement with our ELF results. Therefore, the feature peak in J_{cv} at 21.3 eV is due to interband transitions and is different from the plasmon collective excitation which is observed separately at 23.7 eV in the ELF spectrum. The feature peak at 32 eV in the interband transition

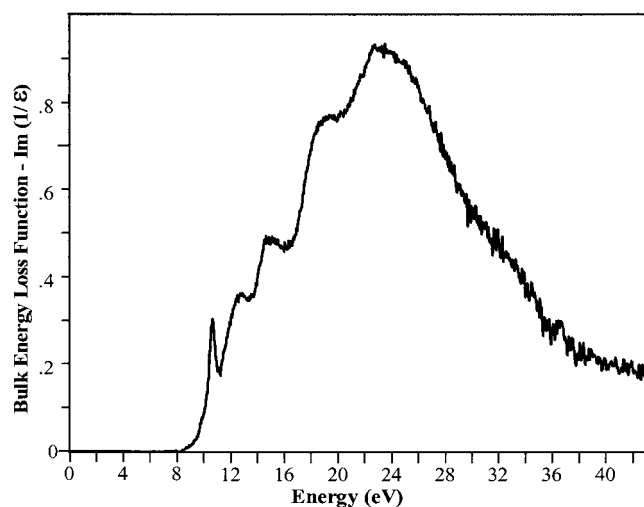


Fig. 10. Bulk electron energy loss function, $-\text{Im}(1/\epsilon)$, of Suprasil 1 amorphous SiO₂, showing a plasmon resonance peak at 23.7 eV.

strength is due to electronic transitions from O 2s energy level to the lower conduction band in SiO₂.

(C) *Sum Rule*: The expected value for the oscillator-strength sum rule for Suprasil 1 amorphous SiO₂ is 16 electrons per SiO₂ formula unit, consisting of eight O 2p electrons, four O 2s electrons, two Si 3s electrons, and two Si 3p electrons. The oscillator-strength sum rule n_{eff} for Suprasil 1 amorphous SiO₂ is shown in Fig. 9, indicating that 9.8 electrons per formula unit, participate in transitions at energies at or below 43 eV. From Fig. 9 we can find a value of 7.3 electrons per SiO₂ formula unit at 26 eV, which is very close to Philipp's¹⁷ 7.7 electrons per SiO₂ molecule near 26 eV. There is no direct evidence that this plot will saturate near 43 eV. Presumably transitions associated with the deeper-lying L-shell electrons of oxygen will be energetically possible at some higher energy and the curve will rise further. It is interesting to note that the reflectance values shown in Fig. 4 for Suprasil 1 amorphous SiO₂ are dropping very fast between the region of 10.4 to 22 eV, indicating that ϵ_2 is decreasing rapidly within this region as shown in Fig. 7. It is assumed that this indicates the exhaustion of oscillator strength for transitions involving the 10 electrons involved in the five Si-O bonds of the SiO₂ tetrahedra.¹⁷

(2) Dispersion Forces with Amorphous SiO₂

(A) *Calculation of $\epsilon_2(\xi)$ Spectra*: Once the complex optical properties as a function of the real frequency ω have been determined, the London dispersion (LD) integral transform (Eq. (3)) must be applied. The LD transform requires data over an infinite frequency or energy range, and therefore, we use analytical extension to continue the data beyond the experimental data range. We choose power-law wings of the form $\text{Re}[J_{cv}] \propto \omega^{-\alpha}$ on the low energy side of the data and $\text{Re}[J_{cv}] \propto \omega^{-\beta}$ on the high energy side of the data. We have chosen fixed values of $\beta = 3$ and $\alpha = 2$ and wings that are extended to cover from 0 to 250 eV to minimize errors due to neglected areas in the ensuing integrals used in Hamaker constant determination. On determining the LD spectrum, we retain the complete spectrum over the entire 0–250 eV range, not just the limited experimental data range, to facilitate the evaluation of the spectral difference functions while continuing to minimize errors resulting from neglected area between the $\epsilon_2(\xi)$ spectra.

The LD spectrum for SiO₂ calculated from the interband transition strength using the above method is shown in Fig. 11. Once we have determined the complex optical properties and calculated the LD spectra, we can calculate the Hamaker constants for many physical configurations. In the full spectra Hamaker constant method, we typically restrict the range of LD spectra to

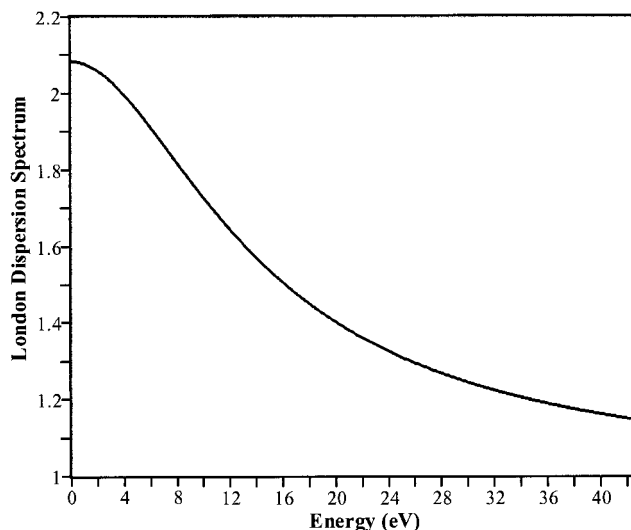


Fig. 11. London dispersion spectrum of Suprasil 1 amorphous SiO₂.

Table II. Hamaker Constant (A_{121}^{NR}) of Suprasil SiO₂, Determined from Interband Transition Spectrum

Physical geometry	A_{121}^{NR} (zJ)
[Suprasil SiO ₂ Vacuum Suprasil SiO ₂]	71.6
[Suprasil SiO ₂ Al ₂ O ₃ Suprasil SiO ₂]	24.6
[Suprasil SiO ₂ Water Suprasil SiO ₂]	8.0
[Suprasil SiO ₂ MgO Suprasil SiO ₂]	7.4
[Suprasil SiO ₂ SiO ₂ Suprasil SiO ₂]	1.1
[Si ₃ N ₄ SiO ₃ Si ₃ N ₄]	38.2
[Suprasil SiO ₂ Water Air]	-15.6

250 eV, whereas the integrals over frequency should extend to infinity. The detailed methods for calculating full spectral of Hamaker constant can be found in French's review article.⁵² Here we report the Hamaker constants for different configurations with amorphous SiO₂ in Table II.

(B) *Hamaker Constant for Different Configurations:* Now let's consider a physical configuration for a Hamaker constant calculation that consists of two layers of Suprasil SiO₂ separated by an interlayer film. For a nonretarded Hamaker constant to apply, the film should be very thin (<2 nm) and can be any kind of material. This model is denoted as a symmetrical 121 structure⁵² and shown in Fig. 12. For this structure, whose interlayer or intergranular film has such different physical properties and electronic structure, it is of interest to determine the magnitude of the London dispersion force. From the VUV spectra of Suprasil 1 amorphous SiO₂ separated from SiO₂ by vacuum (A_{121}^{NR}) is 71.6 zJ (Table II). When an interlayer material of Al₂O₃ separates the two layers of amorphous SiO₂, then the Hamaker constant (A_{121}^{NR}) is reduced from 71.6 to 24.6 zJ (1 zJ = 10⁻²¹ J), corresponding to a reduction in the London dispersion force by a factor of 2.5 due to the presence of this disordered film. For such interlayer materials, as MgO and SiO₂ itself (Table II), then the density, the oscillator strength sum rule, and the index of refraction of the intergranular film would be comparable to the bulk Suprasil layers, and the Hamaker constant (7.4 and 1.1 zJ, respectively) and the London dispersion force at the interlayer approach zero (Table II). For such systems with low optical contrast, the London dispersion force is expected to be negligible, while for disordered boundaries such as Σ 13 interface in SrTiO₃ grains,⁵³ the London dispersion force is larger (83 zJ) than that seen for many ceramic systems such as silica particles in alumina for which the Hamaker constant is 24.6 zJ (Table II). Also the Hamaker constant of 71.6 zJ for amorphous Suprasil SiO₂ under vacuum is larger than the previously reported value of 66 zJ.⁵⁰ When amorphous SiO₂ separates two layers of Si₃N₄, the Hamaker constant is calculated to be 38.2 zJ. For the special case of water on the surface of amorphous SiO₂ and exposed to air, the Hamaker constant becomes negative, approaching -15.6 zJ, corresponding to a wetting condition.

V. Conclusions

Because Kramers-Kronig dispersion analysis of reflectance data is the critical step in accurately determining the optical properties, we have augmented the combining spectroscopic ellipsometry and VUV reflectance spectrum with spectroscopic ellipsometry data to span a wider energy range with an improved

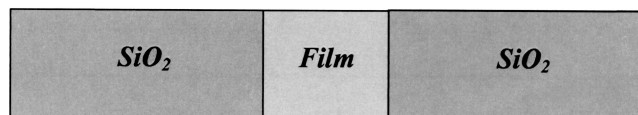


Fig. 12. Configuration of two layers of SiO₂ separated by an interlayer film.

accuracy in amplitude. This has dramatically improved the accuracy in determining the quantitative VUV optical properties for Suprasil 1 amorphous SiO₂ over the range from 0.7 to 43 eV, which is especially important for SiO₂ applications such as candidate materials for photomask lithography at 157 nm. Besides the VUV reflectance spectrum and dielectric constants, we have also derived the complex index of refraction, interband transition strength ($\text{Re}[J_{cv}]$), the oscillator-strength sum rule, the energy loss function, and the London dispersion spectrum for Suprasil 1 amorphous SiO₂ up to 43 eV for the first time. The index of refraction and extinction coefficient values measured from both spectroscopic ellipsometry measurement and Phillip's results agree well with those from VUV reflectance spectrum data within an energy range of 0.7–8 eV. The experimentally determined absorption coefficient, α (cm⁻¹), calculated from the reflectance spectrum for Suprasil 1 SiO₂ fused glass has been evaluated in the energy region of the absorption edge. Band gaps of Suprasil 1 SiO₂ glass within different regions of absorption edge have also been calculated and compared with those values derived from other methods. Besides the features previously reported at 10.4, 11.6, 14.03, and 17.10 eV, new interband transition features have been observed at 21.3 eV along with O 2s transition at 32 eV. We found the bulk plasmon peak to be 23.7 eV in our energy loss function spectrum, which is similar to valence EELS results. The magnitude of the Hamaker constant for SiO₂|Vacuum|SiO₂ is calculated to be 71.6 zJ, which is different from the previously reported value of 66 zJ.

Acknowledgments

The assistance of D. J. Jones with the VUV spectroscopy is appreciated. We are grateful to Dr. L. K. Denoyer for software development.

References

- R. P. Gupta, "Electronic Structure of Crystalline and Amorphous Silicon Dioxide," *Phys. Rev. B*, **32**, 8278–92 (1985).
- W. Y. Ching, "Theory of Amorphous SiO₂ and SiO_x: I, Atomic Structural Models," *Phys. Rev. B*, **26** [12] 6610–21 (1982).
- R. W. G. Wyckoff, *Crystal Structures*, Vol. 1; p. 312. Interscience, New York, 1965.
- D. L. Griscom, "'E' Center in Glassy SiO₂: ¹⁷O, ¹H, and 'Very Weak' ²⁹Si Superhyperfine Structure," *Phys. Rev. B*, **22**, 4192–202 (1980).
- Y. P. Li and W. Y. Ching, "Band Structure of All Polycrystalline Forms of Silicon Dioxide," *Phys. Rev. B*, **31** [4] 2172–78 (1985).
- Y. Yu and W. Y. Ching, "Electronic and Optical Properties of All Polymorphic Forms of Silicon Dioxide," *Phys. Rev. B*, **44**, 11048–59 (1991).
- R. H. French, R. A. Rahme, D. J. Jones, and L. E. McNeil, "Absorption Edge and Band Gap of SiO₂ Fused Silica Glass," *Ceram. Trans.*, **28**, 63–80 (1992).
- N. M. Ravindra and J. Narayan, "Optical Properties of Amorphous Silicon and Silicon Dioxide," *J. Appl. Phys.*, **60** [3] 1139–46 (1986).
- T. M. Bloomstein, M. W. Horn, M. Rothschild, R. R. Kunz, S. T. Palmacci, and R. B. Goodman, "Lithography with 157 nm Lasers," *J. Vac. Sci. Technol., B*, **15**, 2112–16 (1997).
- M. Rothschild, T. M. Bloomstein, J. E. Curtin, D. K. Downs, T. H. Fedynshyn, D. E. Hardy, R. R. Kunz, V. Liberman, J. H. C. Sedlacek, R. S. Uttar, A. K. Bates, and C. V. Peski, "157 nm: Deepest Deep Ultraviolet Yet," *J. Vac. Sci. Technol., B*, **17**, 3262–66 (1999).
- Y. Ikuta, S. Kikugawa, M. Hirano, and H. Hosono, "Defect Formation and Structural Alternation in Modified SiO₂ Glasses by Irradiation with F₂ Laser or ArF Excimer Laser," *J. Vac. Sci. Technol., B*, **18** [6] 2891–95 (2000).
- H. Hosono, M. Mizuguchi, H. Kawazoe, and T. Ogawa, "Effects of Fluorine Dimer Excimer Laser Radiation on the Optical Transmission and Defect Formation of Various Types of Synthetic SiO₂ Glasses," *Appl. Phys. Lett.*, **74** [19] 2755–57 (1999).
- H. Hosono, M. Mizuguchi, and L. Skuja, "Fluorine-Doped SiO₂ Glasses for F₂ Excimer Laser Optics Fluorine Content and Color-Center Formation," *Opt. Lett.*, **24**, 1549 (1999).
- L. A. Moore and C. Smith, "Vacuum Ultraviolet Transmitting Silicate Oxyfluoride Lithography Glass," U.S. Pat. No. US 6 492 072, B2, December 10, 2002.
- L. A. Moore and C. Smith, "Vacuum Ultraviolet Transmitting Silicate Oxyfluoride Lithography Glass," U.S. Pat. No. 6 242 136, B1, June 5, 2001.
- H. R. Philipp, "Optical and Bonding Model for Noncrystalline SiO_x and SiO_xN_y Materials," *J. Non-Cryst. Solids*, **8–10**, 627–32 (1972).
- H. R. Philipp, "Optical Properties of Noncrystalline Si, SiO, SiO_x and SiO₂," *J. Phys. Chem. Solids*, **32**, 1935–45 (1971).
- E. Loh, "Ultraviolet Reflectance of Al₂O₃, SiO₂ and BeO," *Solid State Commun.*, **2**, 269–72 (1964).
- H. R. Philipp, "Optical Transition in Crystalline and Fused Quartz," *Solid State Commun.*, **4**, 73–75 (1966).

- ²⁰O. M. Sorokin and V. A. Blank, "Optical Absorption and External Photoeffect of SiO₂ and Al₂O₃ in the 6–40 eV Energy Region," *Opt. Spectrosc.*, **41** [4] 353–56 (1973).
- ²¹S. T. Pantelides, "The Optical Absorption Spectrum of SiO₂"; in *The Physics of SiO₂ and Its Interfaces*. Edited by S. T. Pantelides. Pergamon Press, New York, 1978.
- ²²C. Bosio, G. Harbeke, W. Czaja, and E. Meier, "Vacuum Ultraviolet Measurements on *c*-SiO₂ and *a*-SiO₂," *Helv. Phys. Acta: Condens. Matter.*, **62**, 748–49 (1989).
- ²³C. Tarrío and S. E. Schnatterly, "Optical Properties of Silicon and Its Oxides," *J. Opt. Soc. Am. B*, **10** [5] 952–57 (1993).
- ²⁴Yu. M. Alexandrov, V. M. Vishbjakov, V. N. Makhov, K. K. Siderin, A. N. Trukhin, and M. N. Ykimenko, "Electronic Properties of Crystalline Quartz Excited by Photons in the 5–25 eV Range," *Nucl. Instrum. Methods Phys. Res., Sect. A*, **282**, 580–82 (1989).
- ²⁵J. E. Rowe, "Photoemission and Electron Energy Loss Spectroscopy of GeO₂ and SiO₂," *Appl. Phys. Lett.*, **25** [10] 576–78 (1974).
- ²⁶S. Loughin, R. H. French, W. Y. Ching, Y. N. Xu, and G. A. Slack, "Electronic Structure of Aluminum Nitride: Theory and Experiment," *Appl. Phys. Lett.*, **63** [9] 1182–84 (1993).
- ²⁷D. J. Jones, R. H. French, H. Muellejans, S. Loughin, A. D. Dorneich, and P. F. Garcia, "Optical Properties of AlN Determined by Vacuum Ultraviolet Spectroscopy and Spectroscopic Ellipsometry Data," *J. Mater. Res.*, **14** [11] 4337–44 (1999).
- ²⁸Heraeus Suprasil Synthetic Glass, Bes Optics, Inc., West Warwick, RI.
- ²⁹Woollam Spectroscopic ellipsometer, J. A. Woollam Co., Inc., Lincoln, NE.
- ³⁰B. Johs, R. H. French, F. D. Kalk, W. A. McGahan, and J. A. Woollam, "Optical Analysis of Complex Multilayer Structures Using Multiple Data Types"; pp. 1098–106 in Proceedings of SPIE—The International Society for Optical Engineering, Vol. 2253, *Optical Interference Coatings*. Edited by F. Abeles. SPIE—The International Society for Optical Engineering, Bellingham, WA, 1994.
- ³¹R. H. French and J. B. Blum, "Electronic Structure and Conductivity of Al₂O₃," *Ceram. Trans.*, **7**, 111–34 (1990).
- ³²M. L. Bortz, R. H. French, "Optical Reflectivity Measurements Using a Laser Plasma Light Source," *Appl. Phys. Lett.*, **55** [19] 1955–57 (1989).
- ³³R. H. French, "Laser-Plasma Sourced, Temperature Dependent VUV Spectrophotometer Using Dispersive Analysis," *Phys. Scr.*, **41** [4] 404–408 (1990).
- ³⁴H. C. Hamaker, "The London–Van der Waals Attraction between Spherical Particles," *Physica*, **4** [10] 1058–72 (1937).
- ³⁵A. D. Dorneich, R. H. French, H. Müllejans, S. Loughin, and M. Rühle, "Quantitative Analysis of Valence Electron Energy-Loss Spectra of Aluminum Nitride," *J. Microsc.*, **191** [3] 286–96 (1998).
- ³⁶H. R. Philipp, "Silicon Dioxide (SiO₂) (Glass)"; pp. 753–63 in *Handbook of Optical Constants of Solids*, Vol. 1. Edited by E. D. Palik. Academic Press, New York, 1985.
- ³⁷D. Y. Smith, "Dispersion Theory, Sum Rules, and Their Application to the Analysis of Optical Data"; pp. 35–68 in *Handbook of Optical Constants of Solids*. Edited by E. D. Palik. Academic Press, New York, 1985.
- ³⁸C. Kittel, *Solid State Physics*, 5th ed.; p. 209. Wiley, New York, 1976.
- ³⁹D. R. Pierce and W. E. Spicer, "Electronic Structure of Amorphous Si from Photoemission and Optical Studies," *Phys. Rev.*, **B5**, 3017–29 (1972).
- ⁴⁰R. Zallen, E. R. Drews, R. L. Emerald, and M. L. Slade, "Electronic Structure of Crystalline and Amorphous As₂S₃ and As₂Se₃," *Phys. Rev. Lett.*, **26**, 1564–67 (1974).
- ⁴¹Z. A. Weinberg, G. W. Rubloff, and E. Bassons, "Transmission, Photoconductivity, and the Experimental Band Gap of Thermally Grown SiO₂ Films," *Phys. Rev. B*, **19**, 3107–17 (1979).
- ⁴²T. H. Distefano and D. E. Eastma, "The Band Edge of Amorphous SiO₂ by Photoinjection and Photoconductivity Measurements," *Solid State Commun.*, **99**, 2259–61 (1971).
- ⁴³D. L. Griscom, "Optical Properties and Structure of Defects in Silica Glass," *J. Ceram. Soc. Jpn.*, **99**, 923–42 (1991).
- ⁴⁴H. Hosono and Y. Ikuta, "Interaction of F₂ Excimer Laser with SiO₂ Glasses: Towards the Third Generation of Synthetic SiO₂ Glasses," *Nucl. Instrum. Methods Phys. Res., Sect. B*, **166–167**, 691–97 (2000).
- ⁴⁵D. L. Griscom, "The Electronic Structure of SiO₂: A Review of Recent Spectroscopic and Theoretical Advances," *J. Non-Cryst. Solids*, **24**, 155–234 (1977).
- ⁴⁶R. B. Laughlin, "Optical Absorption Edge of SiO₂," *Phys. Rev. B*, **22**, 3021–29 (1980).
- ⁴⁷A. J. Bennett and L. M. Roth, "Calculation of the Optical Properties of Amorphous SiO₂ Materials," *Phys. Rev. B*, **4** [8] 2686–96 (1971).
- ⁴⁸H. Ibach and J. E. Rowe, "Electron Orbital Energies of Oxygen Adsorbed on Silicon Surfaces and of Silicon Dioxide," *Phys. Rev. B*, **10**, 710–18 (1974).
- ⁴⁹Y. N. Xu and W. Y. Wing, "Electronic and Optical Properties of All Polymorphic Forms of Silicon Dioxide," *Phys. Rev. B*, **44**, 11048–59 (1991).
- ⁵⁰V. J. Nithianandam and S. E. Schnatterly, "Soft X-ray Emission and Inelastic Electron-Scattering Study of the Electronic Excitations in Amorphous and Crystalline Silicon Dioxide," *Phys. Rev. B*, **38**, 5547–53 (1988).
- ⁵¹A. E. Meixner, P. M. Platzman, and M. Schlueter, "Inelastic Electron Scattering in SiO₂"; p. 85 in *The Physics of SiO₂ and Its Interfaces*. Edited by S. T. Pantelides. Pergamon Press, New York, 1978.
- ⁵²R. H. French, "Origins and Applications of London Dispersion Forces and Hamaker Constants in Ceramics," *J. Am. Ceram. Soc.*, **83** [9] 2117–46 (2000).
- ⁵³K. V. Benthem, R. H. French, W. Sigle, C. Elsaesser, and M. Rühle, "Valence Electron Energy Loss Study of Fe-Doped SrTiO₃ and a Σ13 Boundary: Electronic Structure and Dispersion Forces," *Ultramicroscopy*, **86**, 303–18 (2001). □